NeuroImage 81 (2013) 371–380

Contents lists available at SciVerse ScienceDirect

NeuroImage

journal homepage: www.elsevier.com/locate/ynimg

The challenge of localizing the anterior temporal face area: A possible solution

Vadim Axelrod [a,*], Galit Yovel [a,b]

[a] School of Psychological Sciences, Tel Aviv University, Tel Aviv, Israel
[b] Sagol School of Neuroscience, Tel Aviv University, Tel Aviv, Israel

ARTICLE INFO

Article history:
Accepted 8 May 2013
Available online 17 May 2013

Keywords:
Anterior temporal lobe (ATL)
Face-selective areas
Face recognition
High-resolution fMRI imaging
Multislab scanning method

ABSTRACT

Humans recognize faces exceptionally well. However, the neural correlates of face recognition are still elusive. Accumulated evidence in recent years suggests that the anterior temporal lobe (ATL), in particular face-selective region in the ATL, is a probable locus of face recognition. Unfortunately, functional MRI (fMRI) studies encounter severe signal drop-out in the ventral ATL, where that ATL face area resides. Consequently, all previous studies localized this region in no more than half of the subjects and its volume was relatively small. Thus, a systematic exploration of the properties of the ATL face area is scarce. In the current high-resolution fMRI study we used coronal slice orientation, which permitted us to localize the ATL face area in all the subjects. Furthermore, the volume of the area was much larger than was reported in previous studies. Direct within subjects comparison with data collected with the commonly used axial slice orientation confirmed that the advantage of the coronal slice orientation in revealing a reliable and larger face-selective area in the ATL. Finally, by displaying the face-selective activations resultant from coronal and axial scanning together, we demonstrate an organization principle of a chain of face-selective regions along the posterior–anterior axis in the ventral temporal lobe that is highly reproducible across all subjects. By using the procedure proposed here, a significant progress can be made in studying the neural correlates of face recognition.

Introduction

The anterior temporal lobe (ATL) has been implicated in social and emotional processing as well as in semantic and episodic memory and is therefore of great interest to neurologists and cognitive neuroscientists (Bonner and Price, 2013; Olson et al., 2007; Visser et al., 2009; Wong and Gallate, 2012). In recent years, accumulating evidence suggests that it may also play a key role in face processing and face recognition (for review: Von Der Heide et al., 2013). In particular, the ATL was shown to contain identity information in humans (Anzellotti et al., 2013; Kriegeskorte et al., 2007; Nestor et al., 2008, 2011; Rotshtein et al., 2005) and in macaque monkeys (Eifuku et al., 2004; Eifuku et al., 2011; Freiwald and Tsao, 2010). Impaired activity in the ATL area and disrupted connectivity of this region with posterior occipito-temporal regions were suggested as a possible cause for congenital prosopagnosia (Avidan and Behrmann, 2009; Avidan et al., 2005, 2013). Furthermore, the face-selective portion of the ATL, which has been reported in a few human fMRI studies (Avidan et al., 2013; Nasr and Tootell, 2012; Pinsk et al., 2009; Rajimehr et al., 2009; Tsao et al., 2008) and in fMRI studies of the macaque (e.g. Freiwald and Tsao, 2010; Ku et al., 2011; Tsao et al., 2008) was postulated to play an important role in face recognition. Unfortunately, the ATL, especially its ventral part, suffers from severe fMRI signal drop-out due to magnetic susceptibility caused by the ear canal (Carr et al., 2010; De Panfilis and Schwarzbauer, 2005; Devlin et al., 2000; Gorno-Tempini et al., 2002; Kriegeskorte et al., 2007; Leopold et al., 2006; Olman et al., 2009; Rajimehr et al., 2009). This magnetic field distortion may explain why face-selective activations in the ATL were more reliably found with positron emission tomography (PET) (Sergent et al., 1992) than in fMRI experiments. Indeed, three recent fMRI studies (Pinsk et al., 2009; Rajimehr et al., 2009; Tsao et al., 2008) that explored face-selectivity in the ATL, reported poor activations in this area. In particular, a face-selective response was found in only half of the subjects in Pinsk et al. (2009) (area AT) and in Rajimehr et al. (2009) (area ATFP) and in less than a third of the subjects in Tsao et al. (2008) (area AFP2). Furthermore, the volume of this region was relatively small (less than 75 mm^3 in Tsao et al. (2008) and less than 107 mm^3 in Pinsk et al. (2009)). Given that this area is localized in only a fraction of subjects and its small volume, a systematic and reliable investigation of its functional properties cannot be performed. Consequently, our understanding of the role of the ATL face-area in face recognition is currently limited.

The present study reports a scanning procedure that allows reliable detection of the face-selective ATL in the majority of subjects. Unlike all previous studies, which acquired fMRI data with axial slice orientation, in the current study we used coronal slice orientation. The choice of coronal slice orientation was guided by previous observations that coronal

* Corresponding author at: The Gonda Multidisciplinary Brain Research Center, Bar Ilan University, Ramat Gan 52900, Israel.
E-mail address: vadim.axelrod@gmail.com (V. Axelrod).

1053-8119/$ – see front matter © 2013 Elsevier Inc. All rights reserved.
http://dx.doi.org/10.1016/j.neuroimage.2013.05.015

slice orientation reduces susceptibility artifacts (e.g. O'Doherty et al., 2001; Ojemann et al., 1997; Olman et al., 2009; Whalen et al., 2008). In particular, it has been suggested that coronal slice orientation minimizes signal drop-out by displacing through-plane dephasing, phase cancelation, and phase dispersion (Whalen et al., 2008). Because we used high-resolution scanning (2.08 × 2.08 × 2.4 mm voxel size), a consecutive one-slab scanning did not cover both the anterior and the mid-temporal lobe. Thus, to obtain scanning coverage of face-selective areas in the mid-fusiform gyrus and posterior superior temporal sulcus (STS), the slices were split into two non-consecutive slabs ["multislab" method (Bernstein et al., 2004; Oshio et al., 1991; Posse et al., 2012)]: the anterior slab covered the face areas in the ATL and the posterior slab covered the mid-fusiform gyrus and the STS (see Fig. 1A). In order to estimate whether coronal slice orientation is indeed beneficial for detecting face-selective activations in the anterior temporal lobe, in Experiment 1, we directly compare within subjects data collected with coronal slice orientation with data collected with the standard axial slice orientation. In Experiment 2, we examined the reliability of the activations revealed with coronal orientation by measuring the magnitude of face-selectivity of the ATL face area using data collected from independent scans.

Materials and methods

Apparatus

MRI data were collected using a 3 T GE MRI scanner with an 8-channel head coil. The echo planar imaging sequence used to collect the fMRI data had the following parameters: TR = 2 s, TE = 30 ms, flip angle: 90°, FOV 200 mm, acquisition bandwidth 250 kHZ and slice thickness 2.4 mm (no gap). Acquisition matrix was 96 × 96 (in plane resolution 2.08 × 2.08 mm), which was reconstructed into 128 × 128 matrix (in plane resolution 1.56 × 1.56 mm). In Experiment 1 subjects were scanned using both coronal and axial orientations; in Experiment 2 only the coronal orientation was used. The coronal and axial slice orientations are shown in Figs. 1A and B, respectively. The slice prescription of the coronal orientation was as follows: the anterior slab, which covered the anterior temporal region, was comprised of 13 slices (Experiment 1) and 11 slices (Experiment 2); the posterior slab was comprised of the remaining slices, while the total number of slices varied between subjects from 23 to 25 slices. Anatomical SPGR images were collected with 1 × 1 × 1 mm resolution.

Subjects

Eleven healthy volunteers (age: 24–44, 5 females, all right-handed) participated in Experiment 1. One subject who fell asleep during the scan was excluded from the analysis. Nine healthy volunteers (age: 22–28, 6 females, all right-handed) participated in the Experiment 2. All subjects gave informed consent to participate in the study, which was approved by the ethics committee of the Tel Aviv Sourasky Medical Center.

Stimuli

Experiment 1

All stimuli were color images. The face stimuli were unfamiliar male faces taken from FACES Database (Ebner et al., 2010). Object stimuli were images of tables, taken from various Internet sources. In total there were 32 images of faces and 32 images of tables. The size of the stimuli was 7 × 7° of visual angle.

Experiment 2

Face and object stimuli included grayscale images of famous male faces and cups, taken from various Internet sources. In total there were 16 images of faces and 16 images of cups. The size of the stimuli was 7 × 7° of visual angle.

Design

Design of both experiments was similar. Face and object stimuli were presented in separate blocks (blocked-design). The blocks in each scan were arranged in triplets of face–object–fixation to avoid consecutive presentation of two blocks of the same type. In each scan there were 10 face blocks, 10 object blocks and 10 fixation blocks. The order of face and object blocks was counterbalanced. Duration of stimulus and fixation blocks was 16 s and 8 s respectively. Each stimulus block included 16 trials. Stimulus presentation time was 0.3 s and inter-stimulus interval time was 0.7 s. The total scan duration was 6:52 min. To ensure that subjects paid attention to the stimuli, they were asked to press a

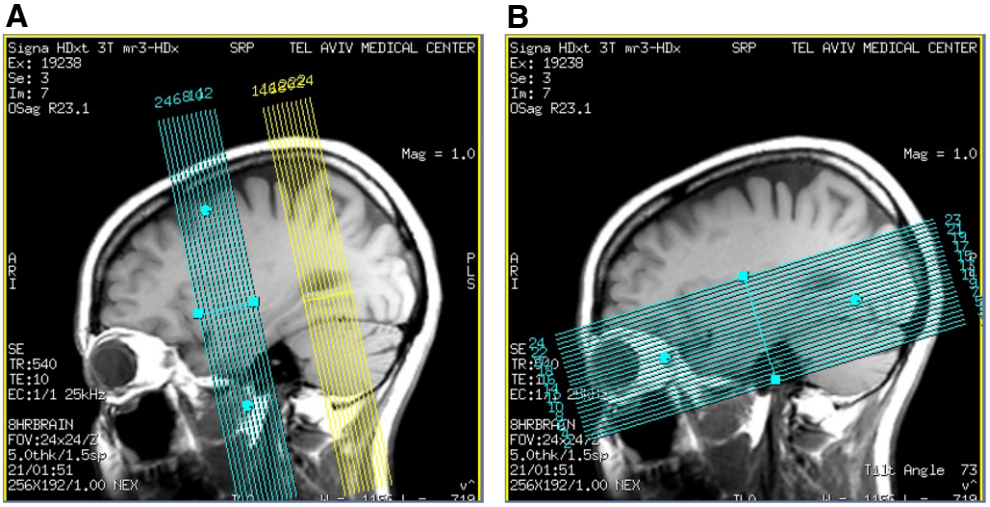

Fig. 1. Slice orientation shown in mid-sagittal view: A. The position of the coronal slices for one representative subject. The anterior slab (blue color) was comprised of 13 slices and covered the anterior temporal region ventrally with parts of the frontal lobes dorsally; posterior slab was comprised of the remaining 10–12 slices and covered mid-temporal areas ventrally and part of the parietal lobe dorsally. B. The position of the commonly used axial orientation slices for one representative subject.

Table 1
Right and left ATL face area: individual subjects MNI coordinates (center of mass) volume for the coronal (left side) and axial (right side) slice orientations.

	Right ATL face Area								Left ATL face Area							
	Coronal slice orientation				Axial slice orientation				Coronal slice orientation				Axial slice orientation			
	MNI coordinates			volume (mm^3)	MNI coordinates			volume (mm^3)	MNI coordinates			volume (mm^3)	MNI coordinates			volume (mm^3)
subject	X	Y	Z		X	Y	Z		X	Y	Z		X	Y	Z	
ai	40	−8	−35	112				0	−31	−11	−41	296				0
aj	35	−12	−35	48	34	−15	−29	40	−36	−12	−30	8	−36	−15	−30	64
az	35	−9	−44	208	43	−16	−35	40	−36	−16	−44	256	−36	−19	−33	320
bs	36	−13	−41	312				0				0				0
ne	32	−12	−40	104				0	−35	−12	−40	168	−37	−11	−31	48
ol	30	−10	−36	448	30	−14	−31	144	−30	−12	−38	224	−32	−12	−38	8
rm	30	−10	−38	8				0	−33	−9	−31	240				0
sk	30	−8	−39	16				0	−35	−7	−39	64				0
sm	33	−8	−35	856	34	−7	−34	336	−34	−10	−28	144	−36	−11	−28	88
vd	34	−6	−45	392	34	−12	−38	144	−40	−13	−28	424	−39	−16	−26	368
Mean	**34**	**−10**	**−39**	**250.4**	**35**	**−13**	**−33**	**70.4**	**−34**	**−11**	**−35**	**182.4**	**−36**	**−14**	**−31**	**89.6**
MSE	**1.01**	**0.7**	**1.17**	**83.45**	**6.67**	**2.74**	**6.26**	**34.64**	**1.01**	**0.7**	**1.17**	**83.45**	**2.14**	**1.59**	**1.57**	**34.64**

response key whenever the same image appeared in two consecutive trials (a one-back task). The number of repetitions varied from block to block (minimum number was zero and maximum number was four). To prevent identity discrimination based on apparent motion, the location of the stimuli varied across trials with a random jitter of 20 pixels (0.35° of visual angle). In Experiment 1 all subjects completed 6 scans (3 coronal and 3 axial orientations). The order of coronal/axial scans was interleaved, while the slice orientation of the first scan was counterbalanced across subjects. In Experiment 2 all subjects completed 5 scans with coronal orientation only.

Data analysis

Preprocessing

SPM5 (Wellcome Department of Imaging Neuroscience, London, UK; www.fil.ion.ucl.ac.uk) was used for data analysis. The functional scans were realigned, motion corrected, normalized to $2 \times 2 \times 2$ voxel resolution using MNI template and smoothed with a FWHM $= 3 \times 3 \times 3$ mm kernel. The normalization was done using a unified segmentation procedure (Ashburner and Friston, 2005). In EPI scans first six volumes (12 s) were discarded from the analysis.

Region of interest analysis

A GLM was estimated for each subject (HRF boxcar function). The GLM was estimated using two regressors one for faces and one for objects. Face-selective areas (fusiform face area [FFA], superior temporal sulcus [STS], ATL face-area, amygdala and the prefrontal cortex) were found using faces > object contrast ($p < 0.001$, uncorrected). Time courses were extracted for each regressor using the MarsBaR region of interest toolbox for SPM (Brett et al., 2002). The peak plateau values (from TR = 4 to TR = 8 from block onset) were averaged and analyzed using SPSS 17.

To establish whether the face-selective ATL voxels are located within gray matter we used gray matter maps from segmentation procedure. Using a custom-made MATLAB code, for each subject individually, the values from gray matter map that corresponded to face-selective ATL ROIs were extracted. Only the voxels with gray matter probability of at least 80% were considered as gray matter voxels.

Time series signal-to-noise ratio (tSNR) (Kruger and Glover, 2001; Weiner and Grill-Spector, 2010) was calculated for each subject based on the first scan (200 volumes) of the experiment (Peelen and Caramazza, 2012) for the scans in coronal and axial slice orientation. The tSNR was calculated in the following way: first, the time course for each voxel of the face-selective ATL was extracted; second, all time courses were averaged resulting in one ROI time course; and third, tSNR was calculated as mean ROI time course value divided by the standard deviation.

Results

Experiment 1

Behavioral results

Average performance on the one-back task (i.e., correct detection of two consecutive images) was 81.5% (MSE: 3.7%) for faces and 72.6% (MSE: 5.3%) for tables. Average correct detection rate was significantly higher for faces comparing to tables (two-tailed t-test, $t(9) = 2.46$, $p = 0.036$).

Functional MRI results

Within subject comparison between coronal and axial slice orientation

The volume and MNI coordinates of face-selective activations in the ATL for coronal and axial slice orientation are reported in Table 1. In line with previous reports (Nasr and Tootell, 2012; Pinsk et al., 2009; Rajimehr et al., 2009) using axial slice orientation the face-selective ATL was found in about half of the subjects only. Five out of 10 subjects showed a right ATL and 6 out of 10 subjects showed a left ATL. Notably, using coronal slice orientation we localized the right ATL face area in all participants and the left ATL face area in 9 out of 10 participants. Furthermore, the volume of the ATL face area using coronal orientation was 2–3 times larger (right hemisphere: 250 mm^3, left hemisphere: 182 mm^3) comparing to the axial orientation (right hemisphere: 70 mm^3, left hemisphere: 90 mm^3) (Table 1, Fig. 2). Paired t-test which compared the volume of the ATL face area across the two scanning orientations revealed significantly larger volume with coronal compared to the axial scanning orientation: right hemisphere [$t(9) = 3.42$, $p < 0.001$, paired t-test, two-tails] and in the left hemisphere [$t(8) = 2.44$, $p = 0.04$, paired t-test, two-tails]; notably, the volume of the ATL face area localized using axial orientation that we found is consistent with previous reports in Tsao et al. (2008) and in Pinsk et al. (2009) that found an ATL face area of less than 100 mm^3. The ATL face-selective activations were mostly located in gray matter: in the right ATL face area 68.9% (SEM = 4.9%) and in the left ATL face area 80.3% (SEM = 7.3%) of the voxels were gray matter voxels.

To test whether the better ATL face-selective activations we obtained using coronal slice orientation were due to higher signal-to-noise compared to axial orientation, we calculated time series signal-to-noise ratio (tSNR) (Kruger and Glover, 2001; Weiner and Grill-Spector, 2010) for coronal and axial slice orientation scanning in the ATL face area that we localized with the coronal slice orientation. Our results show that the values of tSNR in the ATL face area (bilaterally) were higher for coronal than in axial slice orientation (right ATL face area [$t(9) = 2.62$, $p = 0.03$], the left ATL face area [$t(9) = 2.27$, $p = 0.05$]). Fig. 3 shows for one representative subject (subject "az")

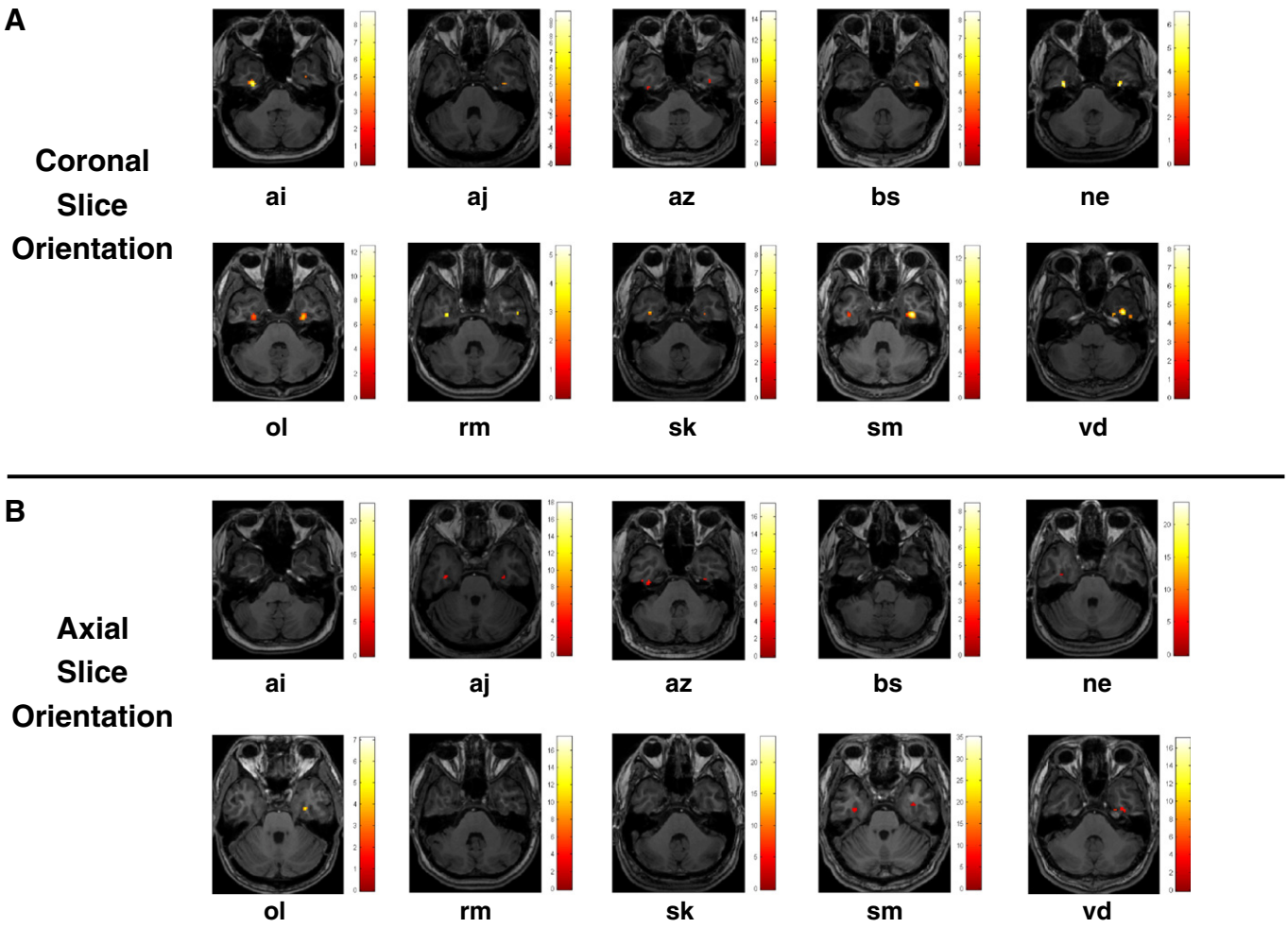

Fig. 2. Individual face-selective activations (faces > tables contrast; $p < 0.001$, uncorrected) localized using coronal slice orientation (A) and axial slice orientation (B) clearly show better localization of the face ATL in the former. The functional activations of each of the coronal and axial scanning were both overlaid on an axial anatomical image for best viewing of ATL face-area. Cross-hair indicates the right ATL face area. Please note that in some cases (e.g. left ATL face-area in subject "vd") the right and left ATL cannot be observed on the same horizontal slice. A complete depiction of the location and volume of the face-selective areas for each subject is reported in Table 1.

the raw EPI volume of the two slabs that were collected in the coronal orientation scanning. Face-selective activations are overlaid on the EPI volume. The good quality of the signal at the location of the face-selective ATL can be seen.

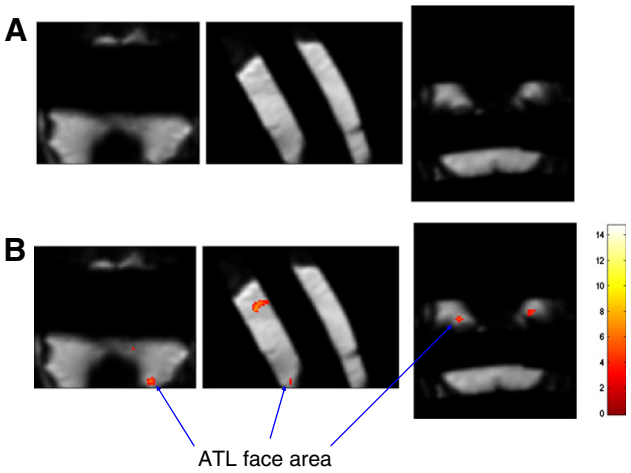

Fig. 3. A. Raw EPI volume of the two slabs that were collected during coronal orientation scanning for a representative subject (subject "az"). B. The same raw EPI volume with overlaid face-selective activations. Note the good quality of the signal in the location of the in the ATL face area (pointed by the arrows).

The effect of number of face object blocks in localizing the ATL face area

It has been recently suggested that a large number of face and object blocks (50–70 blocks) is needed in order to obtain face-selective activations in the ATL (Rajimehr et al., 2009). To test the effect of the number

Table 2
The volume of the left and right ATL face areas in each subject as a function of number of blocks per condition. For example, 10 blocks per condition (second column of the table) means that there were 10 blocks of face stimuli and 10 blocks of object stimuli.

ID	Right ATL face area			Left ATL face area		
	10 blocks (mm^3)	20 blocks (mm^3)	30 blocks (mm^3)	10 blocks (mm^3)	20 blocks (mm^3)	30 blocks (mm^3)
ai	0	0	112	56	184	296
aj	16	40	48	0	0	8
az	32	176	208	128	144	256
bs	64	248	312	0	0	0
ne	0	88	104	0	152	168
ol	80	280	448	16	104	224
rm	0	0	8	152	144	240
sk	0	0	16	0	0	64
sm	448	688	856	88	120	144
vd	96	200	392	232	416	424
Mean	**73.6**	**172**	**250.4**	**67.2**	**126.4**	**182.4**
MSE	**43.14**	**66.48**	**83.45**	**25.67**	**39.01**	**42.31**

Table 3
Volume and coordinates (center of mass) of the ATL face area, prefrontal face area, FFA, STS and amygdala averaged across subjects.

Region	Number of subjects	Average volume (mm^3)	MNI coordinates		
			X	Y	Z
Left ATL face area	9	182	−34	−11	−35
Right ATL face area	10	250	34	−10	−39
Left FFA	10	2001	−41	−59	−20
Right FFA	10	3451	40	−56	−20
Left prefrontal	6	1840	−43	18	25
Right prefrontal	9	3184	48	18	31
Left STS	8	1800	−53	−57	8
Right STS	10	1704	52	−51	8
Left amygdala	9	264	−18	−3	−13
Right amygdala	9	360	18	−3	−14

of blocks per condition on the volume of the ATL face area, we compared the volume of the right ATL face area based on data from one scan (10 blocks per condition), two scans (20 blocks per condition) and three scans (30 blocks per condition). Table 2 shows that the face ATL is found in all subjects only when 30 blocks per condition are used. Yet, in contrast to Rajimehr et al. (2009) that have used 50–70 blocks and a more liberal statistical threshold ($p < .01$) than we used ($p < 0.001$) to localize the ATL face area, our data show that 30 blocks can reveal the ATL face areas with coronal slice orientation. Thus, increasing the number of experimental blocks per se is not sufficient for successful detection of the ATL face area. It is noteworthy, however, that relative to the more posterior face areas (reported below) more repetitions are needed to reliably localize the ATL face area in all subjects, even when coronal orientation scanning is used.

Localizing additional face-selective areas using multislab scanning

In addition to the ATL face area, we were interested in localizing face-selective activations in the middle part of the temporal lobe (mid-fusiform gyrus (FFA) and posterior STS). Yet, the high-resolution scanning together with coronal slice orientation with a focus on the anterior temporal lobe (24–25 slices per subject of 2.4 mm width without gap) significantly limits brain coverage and excludes most areas of the posterior face network. Therefore, we employed a scanning protocol of two slabs with a gap in between them (Fig. 1A): Thirteen first slices covered the anterior temporal region ventrally with parts of the frontal lobes dorsally and the remaining 10–12 slices covered mid-temporal areas ventrally and part of the parietal lobe dorsally. Using this slice prescription, we were able to localize bilateral FFA and right STS face area in all subjects (Table 3). Furthermore, the central part of the anterior slab covered also the amygdala, which permitted to localize amygdala face-selective activations (Ishai et al., 2005) in almost all the subjects (Table 3). Finally, as the dorsal part of the anterior slab covered the prefrontal cortex and this permitted localizing the lateral prefrontal face-selective region (Tsao et al., 2008; see also Ishai et al., 2005) in most of the subjects as well (Table 3). This region is relatively poorly explored probably because it cannot be detected with standard low-resolution scanning (in Tsao et al. (2008) it was detected in only 3 subjects) and it is not covered in most studies of face-selective areas that have been using the axial orientation with high resolution (e.g.: Axelrod and Yovel, 2012; Grill-Spector et al., 2006; O'Craven and Kanwisher, 2000; Sterzer et al., 2008). Given that we detected a relatively large activation in this area in 9 out of 10 subjects over the right hemisphere (6 subjects over the left hemisphere) may suggest that high-resolution scanning is required for reliable detection of this prefrontal area. Future studies will need to systematically reveal what are the best parameters required for studying this area, which, similar to the ATL face area, is also likely to play important role in high-level processing of faces including semantic information related to faces as well as the representation of familiar faces.

Table 4
The volume of the left and right FFA in each subject as a function of number of blocks per condition. For example, 10 blocks per condition (second column of the table) means that there were 10 blocks of face stimuli and 10 blocks of object stimuli.

ID	Right FFA			Left FFA		
	10 blocks (mm^3)	20 blocks (mm^3)	30 blocks (mm^3)	10 blocks (mm^3)	20 blocks (mm^3)	30 blocks (mm^3)
ai	2488	3832	4168	120	352	440
aj	1376	2064	2176	552	768	888
az	968	1472	1600	728	1672	1880
bs	784	1312	1880	16	112	176
ne	2808	3264	4120	944	1192	2352
ol	3984	5000	5920	2280	2664	3976
rm	3112	2824	3320	1960	2000	1968
sk	1592	2360	2920	408	1272	2176
sm	3632	4424	4872	2816	3320	3728
vd	2872	3408	3536	1960	2368	2504
Mean	**2361.6**	**2996**	**3451.2**	**1178.4**	**1572**	**2008.8**
MSE	**354.02**	**386.68**	**433.37**	**313.26**	**326.18**	**398.77**

Similar to the ATL face-area we were interested whether localization of other face-selective regions will benefit from larger number of scanning blocks. The results of the bilateral FFA are presented in Table 4 and we can clearly see that for all subjects (with a single exception) the volume of the FFA increased as a function of the number of blocks.

The main motivation for using coronal slice orientation was to improve fMRI BOLD signal in the anterior temporal lobe and subsequently to reveal the activations of the ATL face-area. Thus, there was no reason to expect that this orientation would be beneficial for localization of activations in brain volumes located in regions that do not suffer from susceptibly artifacts. Yet, to test this empirically we compared the volume of the bilateral posterior STS face area, which was localized using coronal and axial slice orientation. We choose the STS face area, but not the FFA for this comparison because the axial slice orientation included face-selective voxels in the temporal lobe posterior to the ear canal that were not included in the multi-slab coronal slice scanning, in which we skipped this area of the brain (Fig. 1A). For both right and left STS there was no significant difference between average ROI size localized using different slice orientation (two-tail t-test, $t < 1$). Average volume of the left STS using axial orientation was 1928 mm^3 (MSE: 671 mm^3) and using coronal orientation it was 1800 mm^3 (MSE: 649 mm^3); average size of the right STS using axial orientation was 2016 mm^3 (MSE: 400 mm^3) and using coronal orientation it was 1704 mm^3 (MSE: 403 mm^3).

Functional organization of face-selective areas in the temporal lobe

The complementary data that we obtained from the two scanning orientations allows us to explore the organization of face-selective regions along the posterior–anterior axis in the occipito-temporal cortex. To that end we combined the activations resultant from axial orientation scanning and the anterior slab of the coronal orientation scans. For this analysis we did not use posterior slab of coronal orientation scan as axial orientation provided better coverage of the posterior temporal lobe (see Fig. 1). Using this approach we were able to benefit from reliable face-selective activations in the anterior temporal lobe (coronal orientation) and face-selective activations in the more posterior temporal and occipital regions (axial orientation) that cannot be covered with high-resolution coronal slices. Critically, since the anterior temporal lobe was covered by both scanning orientations, we ensured that the voxels that were found with both scanning orientations have been taken only once using the coronal orientation. The results of individual subjects ($p < 0.001$, uncorrected) are shown in Fig. 4 (right hemisphere) and in Fig. 5 (left hemisphere). We can clearly see a chain of face-selective activations (best observed on the sagittal plane), which starts with the OFA and ends with ATL face area, while the FFA is in the middle. It is noteworthy that while the concept of chain of face-selective regions was proposed

beforehand, empirically, it was not demonstrated consistently across all participants (e.g.: Tsao et al., 2008). Here, importantly, we show that this organization principle is reproducible across all participants (more pronounced in the right hemisphere, but can be clearly observed in the left hemisphere as well). A few recent studies have reported additional face areas between the FFA and the ATL face area (AFP1 in Tsao et al., 2008, mid-fusiform in Weiner and Grill-Spector, 2010, 2012, FFA-2 in McGugin et al., 2012; Pinsk et al., 2009). Though coordinates of those regions vary between studies its approximate coordinate on anterior–posterior (Y) axis is about −40 (MNI, center of ROI). In our study we found a cluster of activity more anterior to the FFA (Figs. 4 and 5), which could not be separated from the FFA in most subjects. The most anterior part of this cluster was about −30 on anterior–posterior (Y) axis, which is well in line with regions found anterior to the FFA but posterior to the ear canal in previous studies (McGugin et al., 2012; Pinsk et al., 2009; Tsao et al., 2008; Weiner and Grill-Spector, 2010). Taken together these results clearly show a long posterior–anterior chain of face-selective regions (OFA, FFA (or FFA1 + FFA2 + AFP1), ATL face-area) along the occipito-temporal ventral cortex.

Experiment 2

The goal of Experiment 2 was to test the reliability of the ATL face-selective activations measured with coronal slice orientation across scans by localizing the area using first three scans (30 blocks per condition) and measure face selectivity using remaining two scans (20 blocks per condition).

Behavioral results

Average performance on the one-back task (correct detection of two consecutive images) was 81.6% (MSE: 2.8%) for faces and 71.5% (MSE: 4.8%) for cups. Average performance was significantly higher for faces comparing to cups (two-tailed t-test, $t(8) = 4.66$, $p = 0.0016$).

Functional MRI results

The right ATL face area was localized in 8 (out of 9) subjects (average size: 307 mm^3, MSE: 47.2 mm^3) and left ATL face area was localized in 7 (out of 9) subjects (average size: 71 mm^3, MSE: 17.2 mm^3). Using independent data, time courses for faces and cups were extracted (Figs. 6A and B): average percent signal change for faces was significantly higher than for objects in the right ATL face area [$t(7) = 2.38$, $p = 0.022$] and left ATL face area [$t(6) = 2.55$, $p = 0.043$]. Thus, results suggest that activations in the ATL face area, localized using coronal slice orientation are reliable and reproducible across scans.

General discussion

The goal of this study was to localize the ATL face area with a scanning procedure that allows better detection of this region. The ATL face area, which was suggested to play an important role in face recognition (e.g. Avidan et al., 2005; Kriegeskorte et al., 2007; Nasr and Tootell, 2012; Pyles et al., 2013; Rotshtein et al., 2005; Tsao et al., 2008), has been typically overlooked in most fMRI studies due to significant signal drop-out in this area of the brain, which prevented detection of a reliable face-selective activation in most subjects. Here we show that the use of a coronal slice orientation significantly improves the ability to localize the ATL face area relative to a commonly used axial slice orientation. Notably, using coronal orientation in two experiments we were able to reveal this region in 95% of the subjects in the right hemisphere and in 84% of subjects in the left hemisphere. Furthermore, the volume of the ATL face area localized with coronal orientation was significantly larger relative to the axial orientation within the same subject (Table 1), and indeed more than two times larger than was reported by previous studies that have used a standard, axial slice orientation (Pinsk et al., 2009; Rajimehr et al., 2009; Tsao et al., 2008). Finally, examination of face-selectivity with an independent data set showed that face-selectivity in the ATL face area was reliable and reproducible across scans. Taken together, using the proposed scanning approach significant progress can be made in understanding the role of the ATL face area in face recognition.

The coronal slice orientation was suggested to minimize signal drop-out by through-plane signal dephasing (Kim et al., 2003, 2004; Somerville et al., 2004). Indeed, it was previously used to decrease signal drop-out in the inferior lateral temporal lobe (Ojemann et al., 1997), amygdala (Chen et al., 2003; der Zwaag et al., 2012; e.g. Johnstone et al., 2005; Kim et al., 2003, 2004; Merboldt et al., 2001; Robinson et al., 2004; Somerville et al., 2004; Whalen et al., 2008), orbitofrontal cortex (O'Doherty et al., 2001) and medial temporal lobe (Olman et al., 2009). It is noteworthy, that although the coronal slice orientation was clearly a dominant factor for successful ATL face area localization, we also employed a series of additional scanning optimizations to minimize signal drop-out in the ventral anterior temporal lobe. First, in order to reduce the effect of signal drop-out we used high-resolution scanning (2.08×2.08 mm in-plane, 2.4 mm slice sickness). The reduction of slice thickness is known to decrease signal drop-out, which results from variations in the static magnetic field (B0) within a voxel (Carlin et al., 2011; Farzaneh et al., 1990; Olman et al., 2009) and through-slice dephasing (Jorge et al., 2013). Second, we used a relatively short time to echo (TE) = 30 ms parameter, which is also known to decrease signal drop-out (Farzaneh et al., 1990; Olman et al., 2009). Notably, previous studies that reported face-selective activation in the ATL (Pinsk et al., 2009; Rajimehr et al., 2009; Tsao et al., 2008) also used short TE. However, short TEs are also used in many other fMRI studies that do not report face areas in the ATL as well as in our axial scanning (e.g. Andrews et al., 2010; Nestor et al., 2011; Pitcher et al., 2011). Thus, a short TE by itself does not guarantee successful localization of the ATL face area. Finally, it was important to run 30 blocks per condition in order to achieve successful localization of the ATL face area (Table 2). Whereas, a large number of blocks per condition results in more reliable activations in all brain areas regardless of signal drop-out (Kawabata Duncan and Devlin, 2011), the use of a large number of blocks alone, is not enough. That is, Rajimehr and collegues (Rajimehr et al., 2009; see also: Nasr and Tootell, 2012) presented over 50 blocks per condition and found the ATL face area in only half of the subjects and its volume was smaller than in our study despite using a lower statistical threshold than the one we applied here. It is noteworthy, that given that all aforementioned scanning optimizations were applied for both coronal and axial slice, we can confidently assert that coronal slice orientation plays a critical role in reliable detection of the ATL face area in almost all individuals.

Additional novel aspect of our study was the use of a multislab method to improve brain coverage of high resolution functional MRI scanning (Fig. 1A) (Bernstein et al., 2004; Oshio et al., 1991). One recent functional MRI study also used this method (Posse et al., 2012) for improving temporal resolution and BOLD sensitivity in echo-volumar imaging (EVI) rather than for getting better coverage. The use of a multislab method allowed us to achieve coverage of mid-temporal cortex where additional face areas are typically found. Although it did not allow us to cover the occipital face area (OFA), we did successfully localize the largest posterior-temporal face-selective areas(FFA, pSTS; see Table 3), which would have been impossible had we scanned with one slab (high-resolution scanning with a 2.4 mm slice thickness results in a limited brain coverage). More generally, we believe that

Fig. 4. Combined activations (faces > tables contrast; $p < 0.001$, uncorrected) of the coronal and axial orientation scanning shows a long chain of face-selective areas in the right hemisphere. This includes activations detected by the anterior slab of the coronal scanning combined with the axial scanning. Voxels from axial orientation were taken only in case that they were not included in the coronal (anterior) slab mask. Thus, the resultant image contained non-overlapping results of axial and coronal models. A chain of face-selective regions along the anterior–posterior ventral temporal lobe can be clearly seen on the sagittal plane (OFA, FFA (FFA1 + FFA2), ATL face-area).

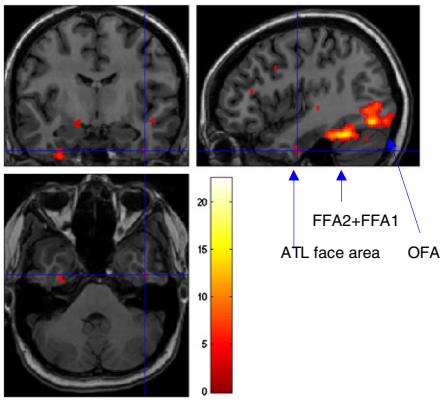

ai

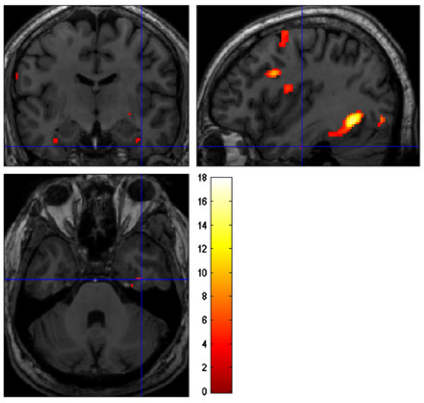

aj

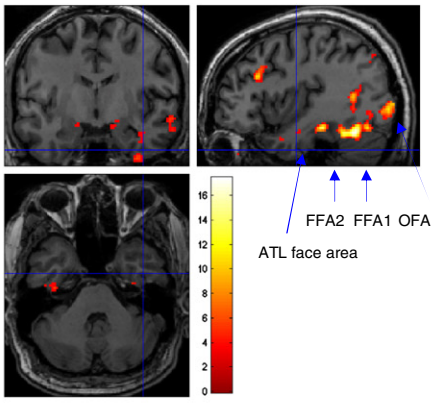

az

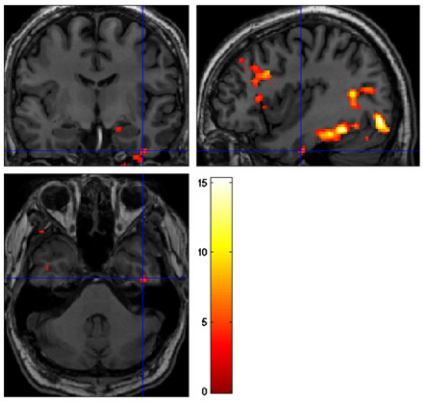

bs

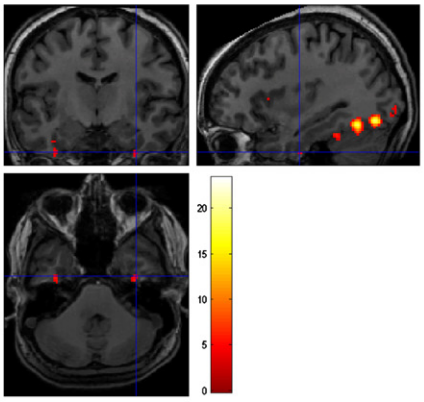

ne

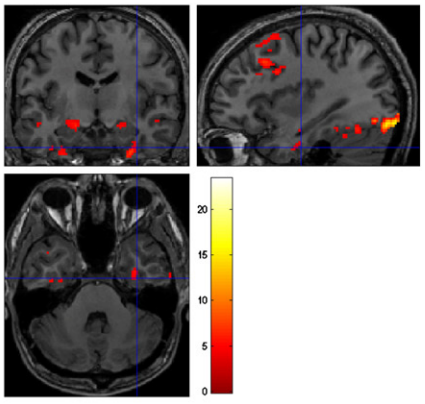

ol

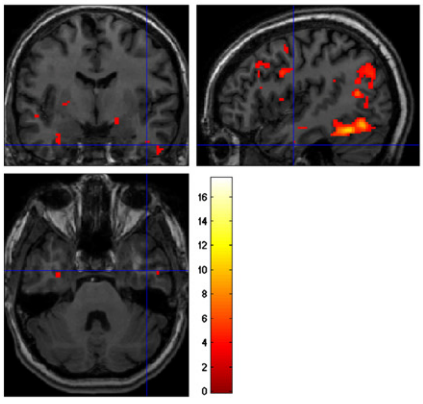

rm

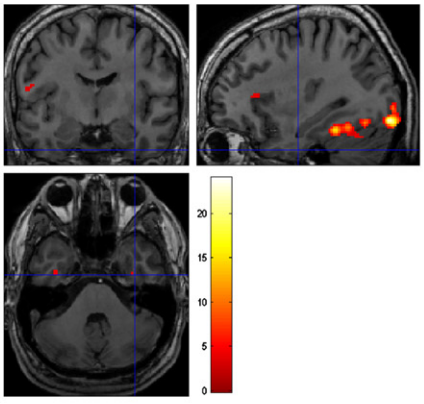

sk

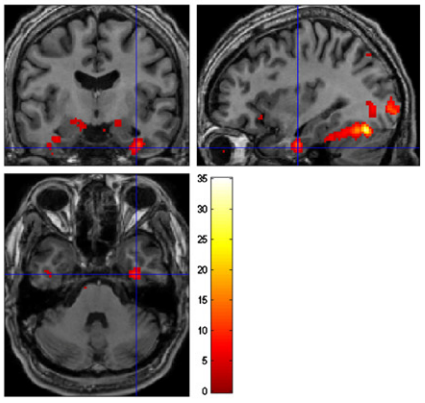

sm

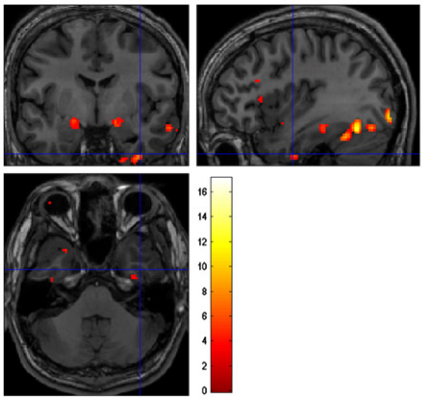

vd

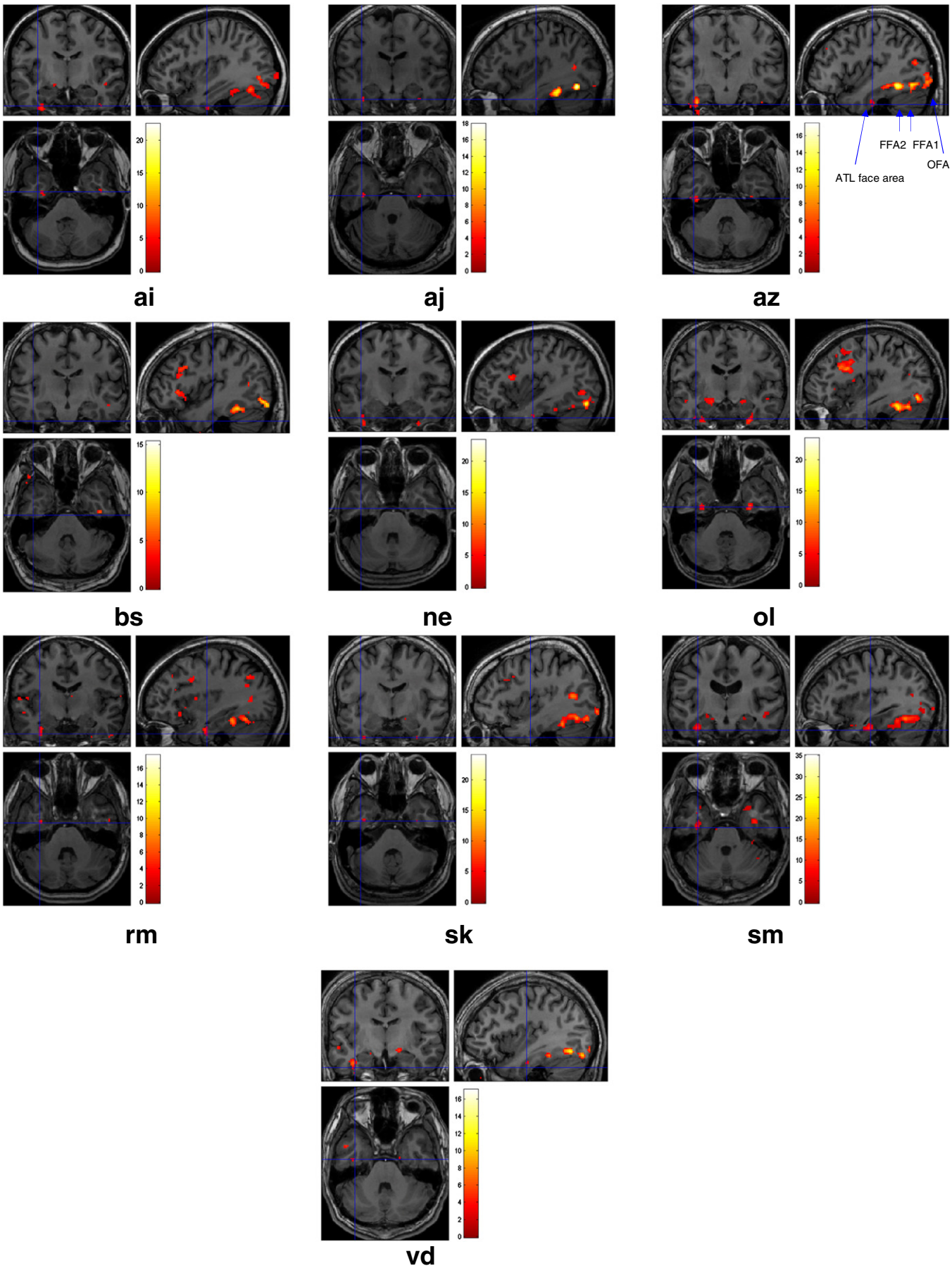

Fig. 5. Combined activations (faces > tables contrast; $p < 0.001$, uncorrected) of the coronal and axial orientation scanning in the left hemisphere.

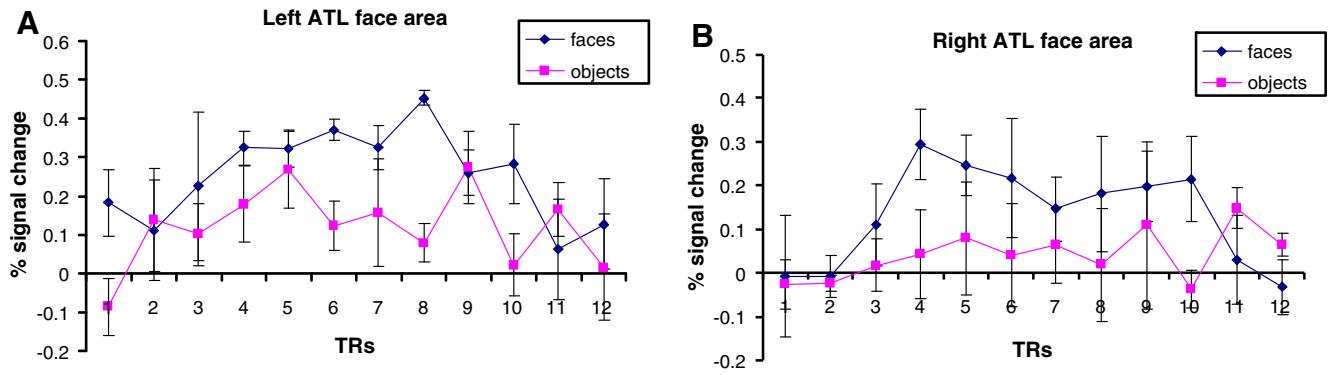

Fig. 6. Face-selectivity results for the ATL face area. (A) Percent signal change for faces and tables in the left ATL face area (average across 8 subjects). Error bars indicate mean standard error. (B) Percent signal change for faces and tables in the right ATL face area (average across 7 subjects). Error bars indicate mean standard error.

the multislab scanning procedure might be beneficial to fMRI high-resolution studies in general, when two distant brain volumes are of interest. For example, high-resolution studies that explore activity in the medial temporal lobe and hippocampus (for review: Carr et al., 2010) can also cover distant areas such as the prefrontal cortex or early visual cortex by using multislab scanning, which are currently overlooked in these studies.

Finally, by combining together the activations from axial and coronal slice orientation scanning we were able to observe a long chain of face-selective areas from the posterior to the anterior temporal lobe, bilaterally in all the subjects (Figs. 4 and 5). Thus, in addition to the commonly found OFA, FFA and STS face area, and the ATL face area we report here and discuss above, most subjects showed at least one additional face-selective areas located anterior to the FFA but posterior to the ATL face-area. This area was recently revealed in a few subjects by several studies (AFP1 in Tsao et al., 2008, mid-Fusiform in Weiner and Grill-Spector, 2010, FFA-2 in McGugin et al., 2012; Pinsk et al., 2009). Interestingly, the anterior face-selective regions are located in the same posterior–anterior axis as the FFA and OFA, suggesting putative mechanism for hierarchical face processing (Freiwald and Tsao, 2010).

Although our main purpose was to reliably detect the ATL face area, the coronal slice orientation scanning also revealed a large face-selective region in the prefrontal cortex. To date only few studies reported this face-selective region (Tsao et al., 2008) and similar to the ATL face-area it was not found in all subjects and its volume was relatively small (but see: Chan and Downing, 2011). Given that face-selective activations in the prefrontal cortex were reliably found in the macaque's brain with both fMRI (Tsao et al., 2008) and single unit recording (Ó Scalaidhe et al., 1997), this area is likely to be an integral part of the face-selective network and to play a critical role in face recognition.

In conclusion, our study demonstrated a reliable procedure for localizing the face-selective area in the ATL using coronal slice orientation. This procedure allows now systematic investigation of the role of this area in face processing, which could not have been accomplished before. We also highlight the application of the multi-slab scanning to obtain better coverage with high-resolution scanning in general. Finally, our results provide important corroboration to the proposal that the anterior temporal face-selective area is an integral part of a large face-processing network.

Acknowledgments

We thank Dafna Ben-Bashat and Moran Artzi for their help with fMRI protocol definition and to Yaniv Assaf for the consultation. We also thank Boaz Sadeh and Ido Tavor for their help with data acquisition. VA was supported by PhD fellowship from the Levi-Edersheim-Gitter Institute for Functional Brain Imaging.

Conflict of interest

The authors declare no conflict of interest.

References

Andrews, T.J., Davies-Thompson, J., Kingstone, A., Young, A.W., 2010. Internal and external features of the face are represented holistically in face-selective regions of visual cortex. J. Neurosci. 30, 3544–3552.
Anzellotti, S., Fairhall, S.L., Caramazza, A., 2013. Decoding representations of face identity that are tolerant to rotation. Cereb. Cortex (http://cercor.oxfordjournals.org/content/early/2013/03/04/cercor.bht046.long).
Ashburner, J., Friston, K.J., 2005. Unified segmentation. NeuroImage 26, 839–851.
Avidan, G., Behrmann, M., 2009. Functional MRI reveals compromised neural integrity of the face processing network in congenital prosopagnosia. Curr. Biol. 19, 1146–1150.
Avidan, G., Hasson, U., Malach, R., Behrmann, M., 2005. Detailed exploration of face-related processing in congenital prosopagnosia: 2. Functional neuroimaging findings. J. Cogn. Neurosci. 17, 1150–1167.
Avidan, G., Tanzer, M., Hadj-Bouziane, F., Liu, N., Ungerleider, L.G., Behrmann, M., 2013. Selective dissociation between core and extended regions of the face processing network in congenital prosopagnosia. Cereb. Cortex (http://cercor.oxfordjournals.org/content/early/2013/01/31/cercor.bht007.full?sid=7d30256b-fb5b-4fb1-8857-74dac764b956).
Axelrod, V., Yovel, G., 2012. Hierarchical processing of face viewpoint in human visual cortex. J. Neurosci. 32, 2442–2452.
Bernstein, M.A., King, K.F., Zhou, X.J., 2004. Handbook of MRI Pulse Sequences, pp. 440–441.
Bonner, M.F., Price, A.R., 2013. Where is the anterior temporal lobe and what does it do? J. Neurosci. 33, 4213–4215.
Brett, M., Anton, J., Valabregue, R., Poline, J., 2002. Region of interest analysis using an SPM toolbox. NeuroImage 1140–1141.
Carlin, J.D., Rowe, J.B., Kriegeskorte, N., Thompson, R., Calder, A.J., 2011. Direction-sensitive codes for observed head turns in human superior temporal sulcus. Cereb. Cortex 44, 735–744.
Carr, V.A., Rissman, J., Wagner, A.D., 2010. Imaging the human medial temporal lobe with high-resolution fMRI. Neuron 65, 298–308.
Chan, A.W.-Y., Downing, P.E., 2011. Faces and eyes in human lateral prefrontal cortex. Front. Hum. Neurosci. 5.
Chen, N.-K., Dickey, C.C., Yoo, S.-S., Guttmann, C.R.G., Panych, L.P., 2003. Selection of voxel size and slice orientation for fMRI in the presence of susceptibility field gradients: application to imaging of the amygdala. NeuroImage 19, 817–825.
De Panfilis, C., Schwarzbauer, C., 2005. Positive or negative blips? The effect of phase encoding scheme on susceptibility-induced signal losses in EPI. NeuroImage 25, 112–121.
der Zwaag, W., Costa, S., Zürcher, N., Adams Jr., R., Hadjikhani, N., 2012. A 7 tesla fMRI study of amygdala responses to fearful faces. Brain Topogr. 25, 125–128.
Devlin, J.T., Russell, R.P., Davis, M.H., Price, C.J., Wilson, J., Moss, H.E., Matthews, P.M., Tyler, L.K., 2000. Susceptibility-induced loss of signal: comparing pet and fMRI on a semantic task. NeuroImage 11, 589–600.
Ebner, N.C., Riediger, M., Lindenberger, U., 2010. Faces—a database of facial expressions in young, middle-aged, and older women and men: development and validation. Behav. Res. Methods 42, 351–362.
Eifuku, S., De Souza, W.C., Tamura, R., Nishijo, H., Ono, T., 2004. Neuronal correlates of face identification in the monkey anterior temporal cortical areas. J. Neurophysiol. 91, 358–371.
Eifuku, S., De Souza, W.C., Nakata, R., Ono, T., Tamura, R., 2011. Neural representations of personally familiar and unfamiliar faces in the anterior inferior temporal cortex of monkeys. PLoS One 6, e18913.
Farzaneh, F., Riederer, S.J., Pelc, N.J., 1990. Analysis of T2 limitations and off-resonance effects on spatial resolution and artifacts in echo-planar imaging. Magn. Reson. Med. 14, 123–139.

Freiwald, W.A., Tsao, D.Y., 2010. Functional compartmentalization and viewpoint generalization within the macaque face-processing system. Science 330, 845–851.
Gorno-Tempini, M.L., Hutton, C., Josephs, O., Deichmann, R., Price, C., Turner, R., 2002. Echo time dependence of bold contrast and susceptibility artifacts. NeuroImage 15, 136–142.
Grill-Spector, K., Sayres, R., Ress, D., 2006. High-resolution imaging reveals highly selective nonface clusters in the fusiform face area. Nat. Neurosci. 9, 1177–1185.
Ishai, A., Schmidt, C.F., Boesiger, P., 2005. Face perception is mediated by a distributed cortical network. Brain Res. Bull. 67, 87–93.
Johnstone, T., Somerville, L.H., Alexander, A.L., Oakes, T.R., Davidson, R.J., Kalin, N.H., Whalen, P.J., 2005. Stability of amygdala bold response to fearful faces over multiple scan sessions. NeuroImage 25, 1112–1123.
Jorge, J., Figueiredo, P., van der Zwaag, W., Marques, J.P., 2013. Signal fluctuations in fMRI data acquired with 2D-EPI and 3D-EPI at 7 tesla. Magn. Reson. Imaging 31, 212–220.
Kawabata Duncan, Keith, J., Devlin, Joseph T., 2011. Improving the reliability of functional localizers. NeuroImage 57 (3), 1022–1030. http://dx.doi.org/10.1016/j.neuroimage.2011.05.009.
Kim, H., Somerville, L.H., Johnstone, T., Alexander, A.L., Whalen, P.J., 2003. Inverse amygdala and medial prefrontal cortex responses to surprised faces. Neuroreport 14, 2317–2322.
Kim, H., Somerville, L.H., Johnstone, T., Polis, S., Alexander, A.L., Shin, L.M., Whalen, P.J., 2004. Contextual modulation of amygdala responsivity to surprised faces. J. Cogn. Neurosci. 16, 1730–1745.
Kriegeskorte, N., Formisano, E., Sorger, B., Goebel, R., 2007. Individual faces elicit distinct response patterns in human anterior temporal cortex. Proc. Natl. Acad. Sci. 104, 20600–20605.
Kruger, G., Glover, G.H., 2001. Physiological noise in oxygenation-sensitive magnetic resonance imaging. Magn. Reson. Med. 46, 631–637.
Ku, S.-P., Tolias, Andreas S., Logothetis, Nikos K., Goense, J., 2011. fMRI of the face-processing network in the ventral temporal lobe of awake and anesthetized macaques. Neuron 70, 352–362.
Leopold, D.A., Bondar, I.V., Giese, M.A., 2006. Norm-based face encoding by single neurons in the monkey inferotemporal cortex. Nature 442, 572–575.
McGugin, R.W., Gatenby, J.C., Gore, J.C., Gauthier, I., 2012. High-resolution imaging of expertise reveals reliable object selectivity in the fusiform face area related to perceptual performance. Proc. Natl. Acad. Sci. 109, 17063–17068.
Merboldt, K.-D., Fransson, P., Bruhn, H., Frahm, J., 2001. Functional MRI of the human amygdala? NeuroImage 14, 253–257.
Nasr, S., Tootell, R.B.H., 2012. Role of fusiform and anterior temporal cortical areas in facial recognition. NeuroImage 63, 1743–1753.
Nestor, A., Vettel, J.M., Tarr, M.J., 2008. Task-specific codes for face recognition: how they shape the neural representation of features for detection and individuation. PLoS One 3, e3978.
Nestor, A., Plaut, D.C., Behrmann, M., 2011. Unraveling the distributed neural code of facial identity through spatiotemporal pattern analysis. Proc. Natl. Acad. Sci. 108 (24), 9998–10003.
Ó Scalaidhe, S.P., Wilson, F.A.W., Goldman-Rakic, P.S., 1997. Areal segregation of face-processing neurons in prefrontal cortex. Science 278, 1135–1138.
O'Craven, K.M., Kanwisher, N., 2000. Mental imagery of faces and places activates corresponding stimulus-specific brain regions. J. Cogn. Neurosci. 12, 1013–1023.
O'Doherty, J., Kringelbach, M.L., Rolls, E.T., Hornak, J., Andrews, C., 2001. Abstract reward and punishment representations in the human orbitofrontal cortex. Nat. Neurosci. 4, 95–102.
Ojemann, J.G., Akbudak, E., Snyder, A.Z., McKinstry, R.C., Raichle, M.E., Conturo, T.E., 1997. Anatomic localization and quantitative analysis of gradient refocused echo-planar fMRI susceptibility artifacts. NeuroImage 6, 156–167.
Olman, C.A., Davachi, L., Inati, S., 2009. Distortion and signal loss in medial temporal lobe. PLoS One 4, e8160.
Olson, I.R., Plotzker, A., Ezzyat, Y., 2007. The enigmatic temporal pole: a review of findings on social and emotional processing. Brain 130, 1718–1731.
Oshio, K., Jolesz, F., Melki, P., Mulkern, R., 1991. T2-weighted thin-section imaging with the multislab three-dimensional rare technique. J. Magn. Reson. Imaging 695–700 (Nov–Dec).
Peelen, M.V., Caramazza, A., 2012. Conceptual object representations in human anterior temporal cortex. J. Neurosci. 32, 15728–15736.
Pinsk, M.A., Arcaro, M., Weiner, K.S., Kalkus, J.F., Inati, S.J., Gross, C.G., Kastner, S., 2009. Neural representations of faces and body parts in macaque and human cortex: a comparative fMRI study. J. Neurophysiol. 101, 2581–2600.
Pitcher, D., Dilks, D.D., Saxe, R.R., Triantafyllou, C., Kanwisher, N., 2011. Differential selectivity for dynamic versus static information in face-selective cortical regions. NeuroImage 56, 2356–2363.
Posse, S., Ackley, E., Mutihac, R., Rick, J., Shane, M., Murray-Krezan, C., Zaitsev, M., Speck, O., 2012. Enhancement of temporal resolution and bold sensitivity in real-time fMRI using multi-slab echo-volumar imaging. NeuroImage 61, 115–130.
Pyles, J.A., Verstynen, T.D., Schneider, W., Tarr, M.J., 2013. Explicating the face perception network with white matter connectivity. PLoS One 8, e61611.
Rajimehr, R., Young, J.C., Tootell, R.B.H., 2009. An anterior temporal face patch in human cortex, predicted by macaque maps. Proc. Natl. Acad. Sci. 106, 1995–2000.
Robinson, S., Windischberger, C., Rauscher, A., Moser, E., 2004. Optimized 3 T EPI of the amygdalae. NeuroImage 22, 203–210.
Rotshtein, P., Henson, R.N.A., Treves, A., Driver, J., Dolan, R.J., 2005. Morphing Marilyn into Maggie dissociates physical and identity face representations in the brain. Nat. Neurosci. 8, 107–113.
Sergent, J., Ohta, S., Macdonald, B., 1992. Functional neuroanatomy of face and object processing. Brain 115, 15–36.
Somerville, L.H., Kim, H., Johnstone, T., Alexander, A.L., Whalen, P.J., 2004. Human amygdala responses during presentation of happy and neutral faces: correlations with state anxiety. Biol. Psychiatry 55, 897–903.
Sterzer, P., Haynes, J.-D., Rees, G., 2008. Fine-scale activity patterns in high-level visual areas encode the category of invisible objects. J. Vis. 8.
Tsao, D.Y., Moeller, S., Freiwald, W.A., 2008. Comparing face patch systems in macaques and humans. Proc. Natl. Acad. Sci. 105, 19514–19519.
Visser, M., Jefferies, E., Lambon Ralph, M.A., 2009. Semantic processing in the anterior temporal lobes: a meta-analysis of the functional neuroimaging literature. J. Cogn. Neurosci. 22, 1083–1094.
Von Der Heide, R.J., Skipper, L.M., Olson, I.R., 2013. Anterior temporal face patches: a meta-analysis and empirical study. Front. Hum. Neurosci. 7.
Weiner, K.S., Grill-Spector, K., 2010. Sparsely-distributed organization of face and limb activations in human ventral temporal cortex. NeuroImage 52, 1559–1573.
Weiner, K., Grill-Spector, K., 2012. Neural representations of faces and limbs neighbor in human high-level visual cortex: evidence for a new organization principle. Psychol. Res. 1–24.
Whalen, P.J., Johnstone, T., Somerville, L.H., Nitschke, J.B., Polis, S., Alexander, A.L., Davidson, R.J., Kalin, N.H., 2008. A functional magnetic resonance imaging predictor of treatment response to venlafaxine in generalized anxiety disorder. Biol. Psychiatry 63, 858–863.
Wong, C., Gallate, J., 2012. The function of the anterior temporal lobe: a review of the empirical evidence. Brain Res. 1449, 94–116.